BioMetals (2005) 18:191–197
DOI 10.1007/s10534-004-6253-y

Characterization of iron compounds in tumour tissue from temporal lobe epilepsy patients using low temperature magnetic methods

Franziska Brem[1,*], Ann M. Hirt[1], Christian Simon[2], Heinz-Gregor Wieser[2] & Jon Dobson[3]

[1]*ETH-Hönggerberg, Institute of Geophysics, CH-8093 Zurich, Switzerland;* [2]*University Hospital Zurich, Neurology/EEG, CH-8091 Zurich, Switzerland;* [3]*Keele University, Institute for Science & Technology in Medicine, Stoke-on-Trent, ST4 7QB, UK; *Author for correspondence (Tel.: +411-633-2626; Fax: +411-633-1065; E-mail: brem@mag.ig.erdw.ethz.ch)*

Received 25 August 2004; accepted 15 December 2004; Published online: March 2005

Key words: biogenic magnetite, brain ferritin, low temperature magnetic measurements, mesial temporal lobe epilepsy (MTLE), tumour tissue

Abstract

Excess iron accumulation in the brain has been shown to be related to a variety of neurodegenerative diseases. However, identification and characterization of iron compounds in human tissue is difficult because concentrations are very low. For the first time, a combination of low temperature magnetic methods was used to characterize iron compounds in tumour tissue from patients with mesial temporal lobe epilepsy (MTLE). Induced magnetization as a function of temperature was measured between 2 and 140 K after cooling in zero-field and after cooling in a 50 mT field. These curves reveal an average blocking temperature for ferritin of 10 K and an anomaly due to magnetite at 48 K. Hysteresis measurements at 5 K show a high coercivity phase that is unsaturated at 7 T, which is typical for ferritin. Magnetite concentration was determined from the saturation remanent magnetization at 77 K. Hysteresis measurements at various temperatures were used to examine the magnetic blocking of magnetite and ferritin. Our results demonstrate that low temperature magnetic measurements provide a useful and sensitive tool for the characterisation of magnetic iron compounds in human tissue.

Introduction

In the brain, iron plays an important role in normal neurological functions such as neurotransmitter synthesis and myelination. It is an essential component of physiological processes, such as oxygen and electron transport, but can also be toxic, acting as a catalyst for the production of free radicals. Many neurodegenerative diseases, such as Alzheimer's and Parkinson's disease, are associated with a disruption of iron metabolism (Beard *et al.* 1993). Iron-induced epilepsy and electrophysiological responses are described in several studies (Ueda *et al.* 1998; Ueda & Willmore 2000) and iron overload may even lead to a predisposition to epilepsy (Ikeda 2001).

The primary iron storage system in most living organisms is in the form of nanoparticles of ferrihydrite ($5Fe_2O_3 \times 9H_2O$) encapsulated by a spherical protein shell. This iron storage protein, ferritin, maintains iron in an available soluble, non-toxic form. Each protein shell of ferritin consists of 24 polypeptide subunits forming an approximately spherical cage of 12 nm in diameter. Potentially toxic ferrous iron is sequestered by the shell and oxidized in the core. The internal cavity has a diameter of approximately 8 nm and is occupied by the ferrihydrite core which undergoes antiferromagnetic ordering at low temperature and has a net magnetic moment arising from frustrated surface spins due to its small size (Massover 1993; Harrison & Arosio 1996;

Chasteen & Harrison 1999; Seehra *et al.* 2000). Many low temperature magnetometry studies have been performed on horse spleen ferritin (Mohie-Eldin *et al.* 1994; Makhlouf *et al.* 1997; Luis *et al.* 1999; Gilles *et al.* 2002) and Dubiel *et al.* (1999) identified ferritin in globus pallidus tissue from the human brain. These authors found that ferritin in the brain had a smaller average core diameter and blocking temperature than ferritin in horse spleen.

Biogenic magnetite is another iron compound that has been identified in human brain tissue (Kirschvink *et al.* 1992; Dobson & Grassi 1996; Schultheiss-Grassi & Dobson 1999; Hautot *et al.* 2003) and in tumour tissue (Kobayashi 1997). Magnetite (Fe_3O_4) is a ferrimagnetic iron oxide with an inverse spinel structure. It contains alternating sublattices of Fe^{2+} and Fe^{3+} ions, which are antiferromagnetically coupled. The alternation of the two sublattices with unequal numbers of unpaired electron spins leads to magnetite's strong ferrimagnetic magnetization. There is preliminary evidence that biogenic magnetite is associated with Alzheimer's disease and some studies have suggested that it may be responsible for the triggering of epileptiform activity (Fuller *et al.* 1995) and the production of free radicals (Schafer *et al.* 2000). Though the source of biogenic magnetite is still unknown, it has been suggested that ferritin may be a precursor for magnetite. If the ferritin protein becomes overloaded or if there is a malfunction in the iron transport channels, a mechanism for Fe^{2+} oxidation is lost (Quintana *et al.* 2000; Dobson 2001; Zhao *et al.* 2003).

Magnetometry methods, which were developed for investigations of magnetic materials, including sediments and rocks, are effective at detecting small concentrations of magnetic iron compounds within diamagnetic and paramagnetic matrices (Maher 1999; Evans 2003). These methods can provide proxy information on the iron compounds that are present in addition to their concentration, and in the case of magnetite, its particle size. Few studies have detected ferritin in the human brain with magnetic methods. The aim of this study is to identify ferritin and biogenic magnetite in brain tumour tissue from mesial temporal lobe epilepsy (MTLE) patients and to determine which magnetic methods are most suitable for the characterisation of these iron oxides in brain tissue.

Material and methods

Two brain tissue samples, GH (gemistocytic astrocytoma, WHO grading II) and NU (ganglioglioma, WHO grading I), were resected from patients with MTLE and immediately frozen at −80 °C. Four types of magnetic measurements were made: (1) acquisition of isothermal remanent magnetization (IRM); (2) thermal demagnetization of low temperature IRM; (3) measurement of induced magnetization (DC susceptibility) as a function of temperature; (4) induced magnetization as a function of field (hysteresis curves). All sample holders, vials, glass ware and surgical instruments used for the sample preparation were soaked in HCl for at least 24 h and rinsed with distilled water to prevent contamination. Precautions were taken to avoid contaminations, as described in earlier studies (Dobson & Grassi 1996), and all samples were weighed prior to measuring.

Acquisition of IRM is useful in identifying ordered, blocked magnetic phases in a material because the measured remanent magnetization is not affected by diamagnetic or paramagnetic materials in the sample, such as tissue and heme iron. For IRM experiments frozen tissue samples were placed in a pre-cooled teflon holder and put into liquid nitrogen. The IRM measurements were done on a 3-axis 2G Enterprises Superconducting Quantum Interference Device (SQUID) with a sensitivity level of 10×10^{-12} Am^2. First, the empty teflon holder was measured at 77 K and then the tissue was placed in the holder and measured in the same manner. The IRM was acquired in an ASC Scientific Pulse Magnetizer Model IM-10–30, where the sample was exposed to a pulsed DC field. First, a pulse of 1 Tesla was applied to the sample and the magnetization was measured. Then, the sample was turned 180° and fields from 10 mT to 1 T were given in the opposite direction. After each pulse, the remanent magnetization in the tissue was measured after 120 s. Afterwards, the tissue was removed and the sample holder was demagnetized in a 150 mT AC field, to remove the acquired IRM. The procedure was repeated for the empty teflon sample holder so that the signal of the holder could then be subtracted from the total IRM signal of the holder and sample.

Thermal demagnetization of low temperature IRM was made on tissue samples that were freeze-dried to remove water. The freeze-dried

tissue was pressed into a cylindrical pellet within a diamagnetic straw using teflon pistons made for this purpose. Thermal demagnetization of low temperature IRM was measured with a Quantum Design Magnetic Property Measurement System (MPMS) SQUID Magnetometer at the University of Bremen. The samples were initially cooled down to 2 K either in the absence of a magnetic field (zero-field cooled, ZFC) or in the presence of a strong 5 T field (field cooled, FC). At 2 K a field of 5 T was applied and then turned off to give an isothermal remanent magnetization. The samples were then heated to 300 K while measuring the magnetic moment in intervals of 2 K. The MPMS is equipped with an internal field compensation coil and has a residual field of less than 100 μT.

Measurements of induced magnetization as a function of temperature or field were also made on a MPMS SQUID magnetometer at the University of Bremen. In the thermal experiments samples were initially cooled to 2 K, either in the absence of a magnetic field (ZFC) or in the presence of a weak 50 mT field (FC). At 2 K a magnetic field of 50 mT was applied and the sample was then heated to 100 K with the magnetic moment measured at intervals of approximately 2 K. Sample magnetization was also measured as a function of field (hysteresis loop) at 5, 25, 77 and 300 K, in fields from −7 to 7 T after cooling the samples in zero field.

Results

Isothermal remanent magnetization (IRM)

All IRM acquisition curves show a rapid increase in magnetization in low fields and saturation is reached by 200 mT (Figure 1). The shape of the curve is suggestive of the ferrimagnetic minerals magnetite and/or maghemite (γ-Fe_2O_3 – an oxidation product of magnetite with slightly smaller saturation magnetization). By giving the samples a saturation magnetization in one direction and then acquiring the IRM in the antipodal direction, it is possible to obtain the coercivity of remanence (H_{cr}). The values are 35 and 25 mT for GH and NU, respectively, and are approximately the same at 77 K and room temperature. A difference in saturation remanence of 7.1×10^{-7} and 3.7×10^{-7} Am^2/kg between the IRM at 300 K and the IRM at 77 K can be seen for GH and NU, respectively, and is due to ultrafine particles in the sample that are superparamagnetic at RT but ferrimagnetic at 77 K.

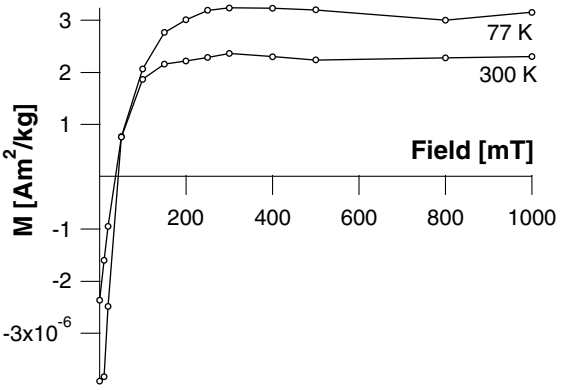

Figure 1. Acquisition of Isothermal Remanent Magnetization (IRM) at 77 and 300 K for sample GH, showing a low coercivity phase and saturation between 200 and 300 mT.

Thermal demagnetization of low temperature isothermal remanent magnetization

The initial IRM intensities of GH and NU at 2 K are 4.5×10^{-4} and 3.3×10^{-4} Am^2/kg, respectively, when cooled in zero field. On heating, there is a sharp decrease in intensity of magnetization between 2 K and 20 K. The field-cooled samples show a higher initial IRM intensity at 2 K of 6.4×10^{-4} for GH and 4.6×10^{-4} Am^2/kg for NU. Again, there is a sharp decrease of magnetization on heating between 2 and 30 K. A slight change in slope is seen in the ZFC curve between 10 and 12 K (Figure 2). For both samples the FC and ZFC curves superimpose indistinguishably at a temperature between 55 and 60 K.

Induced magnetization: DC susceptibility

The measurement of the induced magnetic moment as a function of temperature in a constant field after ZFC or FC is a useful method in the characterization of horse spleen ferritin (Mohie-Eldin *et al.* 1994; Makhlouf *et al.* 1997; Friedman *et al.* 1997; Gilles *et al.* 2000). Figure 3 shows the DC susceptibility as a function of temperature for ZFC and FC. Both curves superimpose above the bifurcation point at approximately 60 K. This

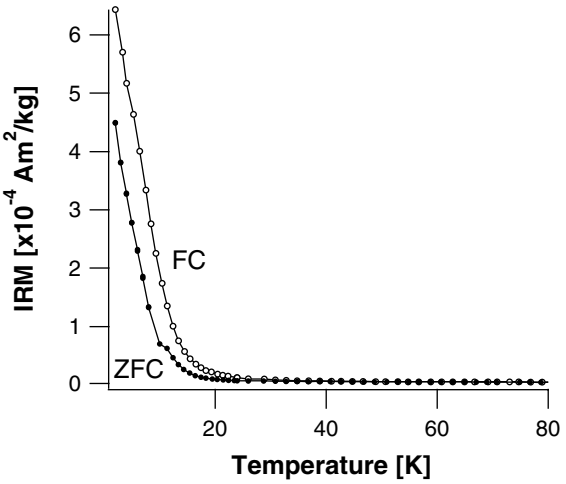

Figure 2. Field cooled (FC) and zero-field cooled (ZFC) thermal demagnetization curves of sample GH.

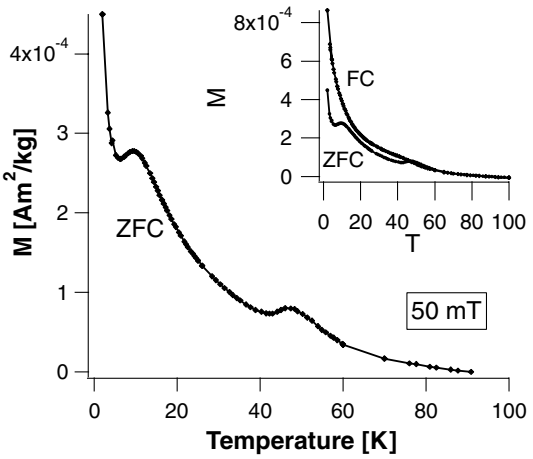

Figure 3. Induced ZFC-magnetization curves as a function of temperature for sample GH between 2 and 100 K in an applied field of 50 mT. The inset shows the FC- and ZFC curves.

point indicates the maximum blocking temperature of the particles in the sample. The FC curve increases rapidly below this temperature, but does not follow the Curie–Weiss law for paramagnetic behaviour. The ZFC curve exhibits two local maxima at 10 and 48 K. The local maximum around 10 K is typical for the magnetic ordering of ferritin in both horse spleen (Makhlouf *et al.* 1997) and the human brain (Dubiel *et al.* 1999). The second local maximum at 48 K is typical for pure magnetite (Walz & Kronmuller 1991; Walz & Kronmuller 1994; Moskowitz *et al.* 1998; Muxworthy 1999). There is a very strong increase in the ZFC curve below 6 K, which suggests further blocking of a magnetic phase; this will be discussed below.

Induced magnetization: hysteresis

The magnetic hysteresis curves are dominated by a strong diamagnetic signal from the tissue also reported by Hautot *et al.* (2003). The diamagnetic signal can be removed from the total signal by subtracting the fit to the curve at 300 K, which is linearly dependent on temperature. Removal of the linear component will also remove any contribution to the magnetization from paramagnetic materials as they also have a linear, albeit positive response. After the removal of the linear components at 300 K, a weak, closed hysteresis loop remains (Figure 4a). The magnetization is saturated by approximately 200 mT, which is typical for magnetite and/or maghemite. The hysteresis at 77 K is similar to the loop at 300 K, but the intensity of the saturation magnetization increases from 7.7×10^{-5} to 7.8×10^{-4} Am^2/kg (Figure 4b). This indicates the further ordering in the low coercivity phase. At 25 K, the hysteresis loop has a contribution from a phase with higher coercivity, which can be attributed to the ordering of ferritin (Figure 4c). The loop is nearly closed, since the average blocking temperature of the ferritin was determined to be 10 K. Therefore, most of the particles in the sample are already in the superparamagnetic state. The lower coercivity phase is still present. The intensity of the magnetization at 7 T is 13×10^{-3} Am^2/kg. At 5 K, the hysteresis loop after ZFC is open and dominated by the ferritin (Figure 5). The magnetization at 7 T is 26×10^{-3} Am^2/kg and the ordered phase has a coercivity of about 50 mT.

Discussion

Both brain samples reveal clearly the presence of two magnetic compounds. Room temperature measurements and the measurements at 77 K are dominated by a low coercivity phase, while at low temperature a high coercivity phase is predominant.

The low coercivity phase at room temperature and 77 K is evident in the results of the IRM measurements and the hysteresis curves and is

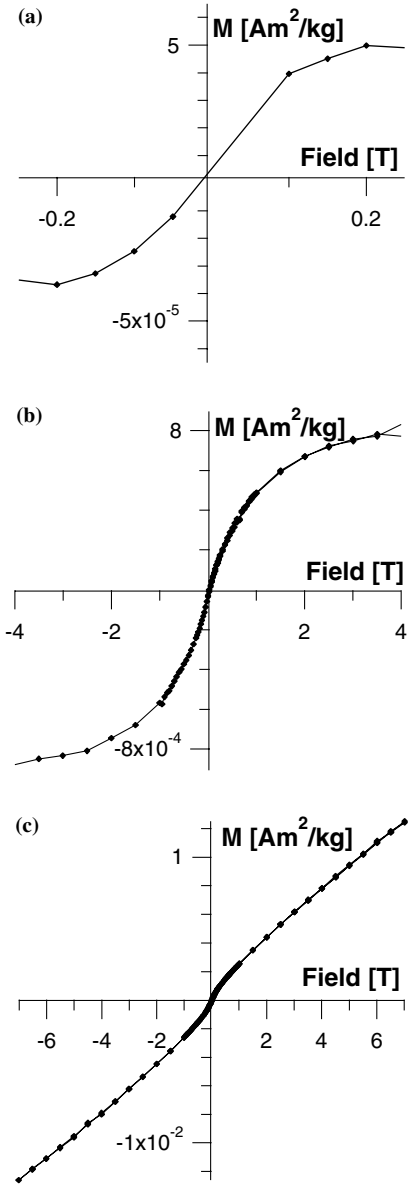

Figure 4. Hysteresis curves from −7 to 7 T of sample GH after subtracting the linear components from the curve. (a) Hysteresis at 300 K, (b) hysteresis at 77 K, (c) hysteresis at 25 K (Note the change in scale).

suggested to be magnetite and/or maghemite. The shape of the IRM curves (Figure 1), typically showing saturation between 200 and 250 mT, and the small remanent coercivity (H_{cr}) between 20 and 30 mT are consistent for either of these materials. Induced magnetization measurements (Figure 3) reveal an anomaly around 50 K that has only been reported for low temperature behaviour in pure

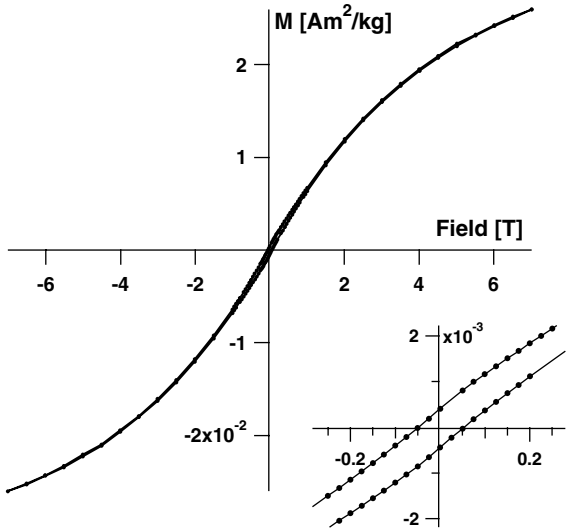

Figure 5. Hysteresis at 5 K from −7 to 7 T of sample GH. The inset shows the coercivity field of 50 mT.

magnetite (Walz & Kronmuller 1991; Walz & Kronmuller 1994; Moskowitz *et al*. 1998; Muxworthy 1999). Assuming that single-domain magnetite is responsible for the magnetization, an estimate of the magnetite concentration of ordered grains in the tissue can be made from the saturation IRM at 77 K, using a value of 46 Am^2/kg for $J_s/2$ (Moskowitz 1993). This value assumes an ensemble of randomly oriented, non-interacting particles. A concentration of 69 and 82 ng/g can be calculated for samples GH and NU, respectively. These values are comparable to earlier studies on magnetite concentration in hippocampus tissue from epileptic patients (Schultheiss-Grassi & Dobson 1999). It should be noted that the estimated concentration is temperature-dependent due to the presence of superparamagnetic grains. Below 77 K, the high coercivity phase becomes predominant, which can be seen in hysteresis measurements at 25 and 5 K (Figures 4c and 5). The hysteresis remains closed at 25 K, even though we see a low coercivity phase in the IRM acquisition curves. This is because the magnetization of the ferritin dominates the induced magnetization at low temperature. The hysteresis at 5 K shows an H_{cr} of 50 mT. There is a strong increase in the magnetization intensity of the high coercivity phase with decreasing temperature. Both curves show no saturation at a field of 7 T. FC and ZFC curves from the thermal demagnetization

measurements decrease rapidly between 2 and 30 K and join between 55 and 60 K (Figure 2). For the induced magnetization measurements, the FC and ZFC curves superimpose also at a temperature of 60 K (Figure 3). The phase shows ordering between 6 and 12 K that causes the local maximum around 10 K.

Results from all three magnetic methods support ferritin as the high coercivity phase. The increase in the contribution to intensity and the increase in coercivity seen in the hysteresis curves, the local maxima found in the ZFC curves of the induced magnetization and thermal demagnetization and the superposition of the ZFC and FC curves are characteristic for ferritin. Hysteresis measurements are very similar to measurements done for horse spleen ferritin. Perfect antiferromagnets (AFM) do not show hysteresis, therefore the open loops are probably due to the switching of frustrated surface spins at the ferritin core or to a defect moment (Néel 1962). The ordering temperature between 6 and 12 K is also typical for ferritin; horse spleen ferritin has an average blocking temperature from 10 to 20 K (Kilcoyne & Cywinski 1995; Makhlouf *et al*. 1997; Friedman *et al*. 1997; Gilles *et al*. 2000). The only magnetic study on human brain ferritin from globus pallidus by Dubiel *et al*. (1999) reports an average blocking temperature of 8.5 K. The distribution of particle volume, energy barriers and therefore blocking temperatures is known from many superparamagnetic systems. At the bifurcation point of FC and ZFC curves, the largest particle in the sample starts to be unblocked and the whole sample is superparamagnetic above 60 K. The FC and ZFC curves of both thermal demagnetization and induced magnetization superimpose at this temperature. This is in agreement with the results reported for horse- and human spleen ferritin by Allen *et al*. (2000).

The strong increase of magnetic moment below 6 K might be due to a paramagnetic phase in the tissue, such as heme iron from blood in the tissue. Blood is reported to show no irregularity in the ZFC curve; the induced magnetization after FC and ZFC superimpose and show a paramagnetic-like decay (Mosiniewicz-Szablewska *et al*. 2003). Similar behaviour of induced magnetization as a function of temperature has been reported for synthetically formed iron-oxyhydroxide cores inside the protein shell apoferritin using sol-gels (Rao *et al*. 2001). An open question is whether the behaviour below 6 K can be due to (1) a mutated ferritin core, which forms a different iron phase or (2) an additional crystalline or non-crystalline phase within the ferritin core. The influence of blood on the magnetic properties at low temperature will be the focus of a future investigation.

Our measurements show that it is possible to obtain consistent results from different methods that support two magnetic phases, ferritin and magnetite, in tumour tissue from human brain resected from the mesial temporal lobe from MTLE patients.

Acknowledgements

We thank the Institute for Geosciences at the University of Bremen, especially Dr. Thomas Frederichs and Prof. Dr. Ulrich Bleil for the use of the MPMS and very helpful discussions. All procedures were approved by the University Hospital-Zurich Medical Ethics Committee. Jon Dobson gratefully acknowledges the support of a Royal Society/Wolfson Foundation Research Merit Award.

References

Allen PD, St Pierre TG, Chua-anusorn W, Strom V, Rao KV. 2000 Low-frequency low-field magnetic susceptibility of ferritin and hemosiderin. *Biochim Biophys Acta-Mol Basis Dis* **1500**, 186–196.

Beard JL, Connor JR, Jones BC. 1993 Iron in the Brain. *Nutr Rev* **51**, 157–170.

Dobson J. 2001 Nanoscale biogenic iron oxides and neurodegenerative disease. *FEBS Lett* **496**, 1–5.

Dobson J, Grassi P. 1996 Magnetic properties of human hippocampal tissue – evaluation of artefact and contamination sources. *Brain Res Bull* **39**, 255–259.

Dubiel SM, Zablotna-Rypien B, Mackey JB, Williams JM. 1999 Magnetic properties of human liver and brain ferritin. *Eur Biophys J Biophys Lett* **28**, 263–267.

Evans ME, Heller F. Environmental magnetism: principals and applications of enviromagnetics, Amsterdam: Academic press.

Friedman JR, Voskoboynik U, Sarachik MP. 1997 Anomalous magnetic relaxation in ferritin. *Phys Rev B* **56**, 10793–10796.

Fuller M, Dobson J, Wieser HG, Moser S. 1995 On the sensitivity of the human brain to magnetic-fields – evocation of epileptiform activity. *Brain Res Bull* **36**, 155–159.

Gilles C, Bonville P, Rakoto H *et al*. 2002 Magnetic hysteresis and superantiferromagnetism in ferritin nanoparticles. *J Magn Magn Mater* **241**, 430–440.

Gilles C, Bonville P, Wong KKW, Mann S. 2000 Non-Langevin behaviour of the uncompensated magnetization

in nanoparticles of artificial ferritin. *Eur Phys J B* **17**, 417–427.

Hautot D, Pankhurst QA, Khan N, Dobson J. 2003 Preliminary evaluation of nanoscale biogenic magnetite in Alzheimer's disease brain tissue. *Proc R Soc Lond Ser B-Biol Sci* **270**, S62–S64.

Ikeda M. 2001 Iron overload without the C282Y mutation in patients with epilepsy. *J Neurol Neurosurg Psychiatry* **70**, 551–553.

Kilcoyne SH, Cywinski R. 1995 Ferritin – a model superparamagnet. *J Magn Magn Mater* **140**, 1466–1467.

Kirschvink JL, Kobayashi-Kirschvink A, Woodford BJ. 1992 Magnetite biomineralization in the human brain. *Proc Natl Acad Sci USA* **89**, 7683–7687.

Kobayashi AK, Yamamoto N, Kirschvink JL. 1997 Studies of inorganic crystals in biological tissue: magnetite in human tumors. *J Jpn Soc Powder Powder metall* **44**, 294–300.

Luis F, del Barco E, Hernandez JM *et al*. 1999 Resonant spin tunneling in small antiferromagnetic particles. *Phys Rev B* **59**, 11837–11846.

Maher BA, Thompson, R. 1999 Quaternary climates, environments and magnetism, Cambridge: Cambridge University Press.

Makhlouf SA, Parker FT, Berkowitz AE. 1997 Magnetic hysteresis anomalies in ferritin. *Phys Rev B* **55**, 14717–14720.

Mohie-Eldin MEY, Frankel RB, Gunther L. 1994 A comparison of the magnetic-properties of polysaccharide iron complex (Pic) and ferritin. *J Magn Magn Mater* **135**, 65–81.

Mosiniewicz-Szablewska E, Slawska-Waniewska A, Swiatek K *et al*. 2003 Electron paramagnetic resonance studies of human liver tissues. *Appl Magn Reson* **24**, 429–435.

Moskowitz BM. 1993 High-temperature magnetostriction of magnetite and titanomagnetites. *J Geophys Res-Solid Earth* **98**, 359–371.

Moskowitz BM, Jackson M, Kissel C. 1998 Low-temperature magnetic behavior of titanomagnetites. *Earth Planet Sci Lett* **157**, 141–149.

Muxworthy AR. 1999 Low-temperature susceptibility and hysteresis of magnetite. *Earth Planet Sci Lett* **169**, 51–58.

Néel L. 1962 Proprietes magnetiques des grains fins antiferromagnetiques – superparamagnetisme et superantiferromagnetisme. *J Phys Soc Jpn* **17**, 676.

Quintana C, Lancin M, Marhic C *et al*. 2000 Initial studies with high resolution TEM and electron energy loss spectroscopy studies of ferritin cores extracted from brains of patients with progressive supranuclear palsy and Alzheimer disease. *Cell Mol Biol* **46**, 807–820.

Rao MS, Dubenko IS, Roy S, Ali N, Dave BC. 2001 Matrix-assisted biomimetic assembly of ferritin core analogues in organosilica sol-gels. *J Am Chem Soc* **123**, 1511–1512.

Schafer FQ, Qian SY, Buettner GR. 2000 Iron and free radical oxidations in cell membranes. *Cell Mol Biol* **46**, 657–662.

Schultheiss-Grassi PP, Dobson J. 1999 Magnetic analysis of human brain tissue. *Biometals* **12**, 67–72.

Seehra MS, Babu VS, Manivannan A, Lynn JW. 2000 Neutron scattering and magnetic studies of ferrihydrite nanoparticles. *Phys Rev B* **61**, 3513–3518.

Ueda Y, Willmore LJ. 2000 Sequential changes in glutamate transporter protein levels during Fe^{3+}-induced epileptogenesis. *Epilepsy Res* **39**, 201–209.

Ueda Y, Willmore LJ, Triggs WJ. 1998 Amygdalar injection of $FeCl_3$ causes spontaneous recurrent seizures. *Exp Neurol* **153**, 123–127.

Walz F, Kronmuller H. 1991 Evidence for a single-stage Verwey-transition in perfect magnetite. *Philos Mag B-Phys Condens Matter Stat Mech Electron Opt Magn Prop* **64**, 623–628.

Walz F, Kronmuller H. 1994 Analysis of magnetic point-defect relaxations in electron-irradiated magnetite. *Phys Status Solidi B-Basic Res* **181**, 485–498.

Zhao GH, Bou-Abdallah F, Arosio P *et al*. 2003 Multiple pathways for mineral core formation in mammalian apoferritin. The role of hydrogen peroxide. *Biochemistry* **42**, 3142–3150.